3-D Finite Element Modelling of a High Pressure Strain Gauge Pressure Transducer

M. H. Orhan*, Ç. Doğan*, H. Kocabaş**, G. Tepehan***

* *TÜBİTAK, Ulusal Metroloji Enstitüsü (UME), Gebze- Kocaeli, Turkey*

** *Istanbul Technical University (ITU), Mech. Eng. Dept., Gümüşsuyu- İstanbul, Turkey*

*** Istanbul Technical University (ITU), Phys. Eng. Dept., Ayazağa- İstanbul, Turkey

Abstract

The scope of this study is a review of the studies on the pressure transducers designed at the TÜBİTAK-UME by utilizing Finite Element Method (FEM) for stress and strain analysis to optimize the design parameters prior to the construction of the pressure transducer prototypes. The constructed and investigated pressure transducer, has a free hardened AISI 4340 steel active element. Hydraulic gauge pressure is applied to the inside and both open ends of this active element. The FEM analysis was conducted by investigating one half of the element in three dimensions and realized at three different pressure values of 60, 100 and 150 MPa. This study presents the FEM output stress and strain values. The validity of those values was established by comparing them with the results obtained from the strain gauge measurements. The relative difference between the two value sets was determined as being lower than 13% of the full scale. The presented results will be helpful for the appropriate design of this kind of pressure transducers using FEM.

1. Introduction

In this study, a strain gauge pressure transducer for hydrostatic gauge pressure measurements up to 150 MPa was constructed on the basis of 'thick-walled cylindrical vessel theory' and stress and strain analysis of the constructed transducer prototypes were realized by using 3-D Finite Element Model (FEM). The sensor of the transducer was chosen as a free active element (a hollow cylinder) considering the fine metrological characteristics reviewed in [1,2]. The design parameters of the sensor were obtained and also optimised by using 3-D FEM. Figure 1 shows a schematic cross section of the transducer and dimensions of the cylindrical active element. Active element was flattened at two opposite side in order to bond strain gauges onto a flat surface. Considering the flattened surface, the ratio of the outer diameter of the cylinder to the inner diameter was made to be approximately between 2.5 and 2.97, in order to have a 2 mV/V output reading

at the maximum applied pressure. Active element and two coupling cups were made of AISI 4340 hardened steel and their hardness were measured and found to be 45-50 HRC. Other essential properties of the material were given in Table 1 [3]. All other components of the transducer were made of 304 stainless steel. The working principle of the transducer could be briefly explained as follows: Hydraulic pressure is applied to the inside and both ends of the free active element by connecting the transducer to the pressure line from its pressure plug (Figure 1). Sealing of the transducer was obtained by means of three pairs of Viton type O-rings having a hardness of 85 Shore. Two strain gauges, model N2A-06-S063Q-350Ω (gauge factor k = 2.09), manufactured by Micromeasurements, were bonded to the centre of the two opposing flat surfaces of the flattened active cylinder. Since the selected strain gauge has a bi-axial rosette pattern, it was possible to measure both circumferential and axial strains [4].

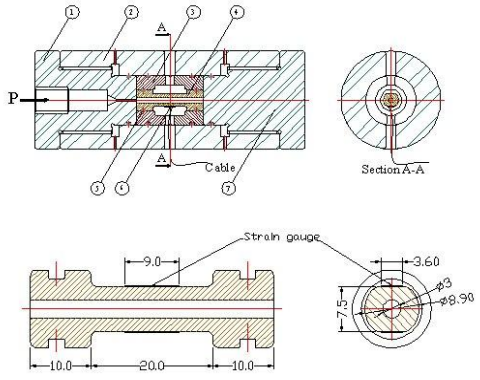

Figure 1. Schematic cross-section diagrams of the pressure transducer: 1. Pressure plug, 2. Outer cylinder, 3. Coupling cup (two pieces), 4. Active element, 5. O-ring, 6. Strain gauge, 7. Blind plug, and dimensions of the active element and the strain gauges.

Uncertainty of the measured pressure value realized by the designed pressure transducer prototype was also evaluated from the calibration results and found to be 0.1 % of the full scale and reviewed in [5]

Table 1. The properties of the material used for the active cylinder and the coupling cup [3]

Material	AISI 4340 Steel
E, Young's modulus (GPa)	207
ν, Poisson's ratio	0.29
Ultimate Tensile Strength (MPa)	1500
Yield Strength (MPa)	1365
α, Linear thermal expansion coefficient ($°K^{-1}$)	11×10^{-6}
Thermal conductivity (W/m°K)	37.4

Additional to the basics of the thick-walled cylinder theory [6], the following assumptions were made to perform the 3-D FEM stress and strain analysis;

1.Elastic properties of the active element are the same in all direction (isotropic material), 2.No body forces on the active element such as gravitational, magnetic, inertia forces, etc. 3.Uniform pressure distributions at inner and outer surfaces of the active element, 4.Hook law was obeyed, 5.Constant axial stress, 6.Cross section perpendicular to the axis remain plane, 7.The pressure inside the O-ring groove was equal to the applied pressure, 8.Tabulated values for modulus of elasticity's and Poisson's ratios supplied by their own manufacturers were true values.

2. FEM Analysis of the Active Element

2.1. The FEM Model

It was decided to utilize 3-D FEM (numerical solution) rather than the analytical

solution [2,6] for the determination of the relation between the applied pressure and the deformation at the flattened surfaces of the active cylinder where the strain gauges were bonded. The symmetrical shape of the transducer and all the design parameters of the active element were selected in such a way as to ensure that a symmetrical stress and strain distribution was obtained even at maximum working pressure of the transducer. Thus, the FEM analysis was conducted by investigating one half of the element in three dimensions and realized at three different pressure values of 60, 100 and 150 MPa.

ANSYS version 5.6.1 FEM software was used to generate the geometrical model and to evaluate the strain values on the area where the strain gauges were bonded. "Solid 45" [7] was used as an element, that was defined by eight nodes having three degrees of freedom each, has translations in the nodal x, y, and z directions and exhibits orthotropic material properties.

A total of 83928 elements and 16415 nodes were used for the complete FEM stress and strain analysis of the active cylinder with grid size 0.5 mm. The FEM model with the applied boundary conditions and the coordinate system were shown in Figure 2.

Considering the working principle and the geometric domain of the transducer, the boundary conditions for the stress and strain analysis were defined in Table 2.

2.2. The FEM Analysis Results

Figure 3 shows the results of FEM analysis for strains in the x and y directions and for the applied pressure of 150 MPa. Figure 4 and 5 show the strain results for the z-direction for the applied pressure of 150 MPa with and without pressurized o-ring groove side, respectively.

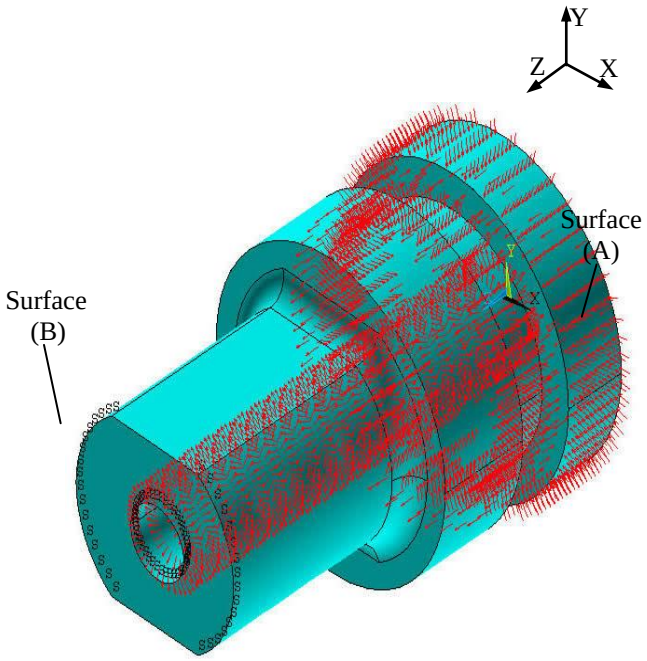

Figure 2. The FEM model with the applied boundary conditions

The strain values on the area where the strain gauges were bonded were plotted with arrows on the gray scaled graphs for the better presentation of the results. The plotted strain values were shown in mm/m.

The results given in Figure 3 and 4 clearly showed that the axial strain was dominant on the electrical output signals of the strain gauge pressure transducer. This was done by selection of the ratio between the areas A and B as approximately 2.

Table 2. Boundary conditions used in FEM model

On the end surface (A)	P(x,y,z) = p	1.5 mm $\leq (x^2 + y^2)^{1/2} \leq$ 6.5 mm	z =0
Inside the active cylinder	P (x,y,z) = p	$(x^2 + y^2)^{1/2}$ = 1.5 mm	0 mm $\leq$ z $\leq$ 20 mm
Symmetric constraint (B)	P (x,y,z) = p	$(x^2 + y^2)^{1/2}$ = 6.5 mm	0 mm $\leq$ z $\leq$ 3.0 mm
On the surfaces of O-ring groove	P (x,y,z) = p	5 mm $\leq (x^2 + y^2)^{1/2} \leq$ 6.5 mm	z = 3.0 mm
	P (x,y,z) = p	$(x^2 + y^2)^{1/2}$ = 5.0 mm	3.0 mm $\leq$ z $\leq$ 5.6 mm
	P (x,y,z) = p	5 mm $\leq (x^2 + y^2)^{1/2} \leq$ 6.5 mm	z = 5.6 mm
p: applied pressure,	$(x^2 + y^2)^{1/2}$: radius of active cylinder,		z axis: axial direction

DMX : Maximum displacement

SMN : Minimum value of the plotted item

SMX : Maximum value of the plotted item

EPTOX : The plotted strain value in X direction

EPTOY : The plotted strain value in Y direction

EPTOZ : The plotted strain value in Z direction

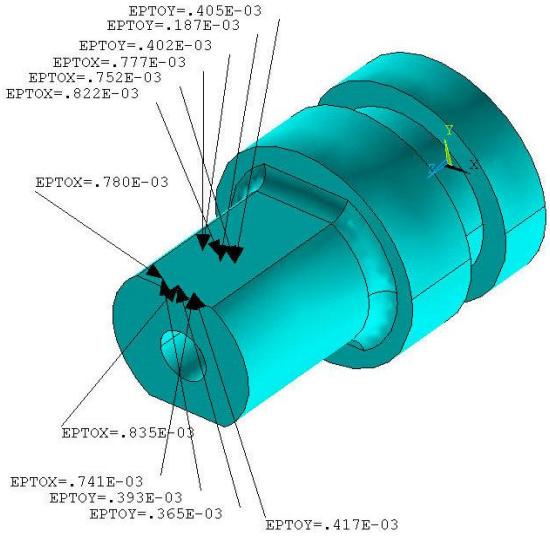

Figure 3. FEM strain results in x and y directions at p = 150 MPa for the pressurized o-ring groove side.

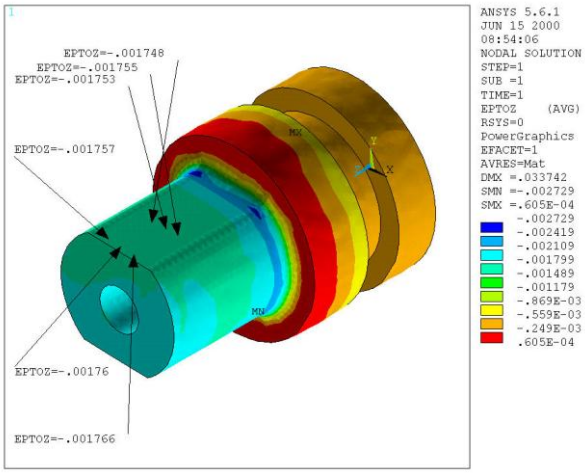

Figure 4. FEM strain results in z-direction at p = 150 MPa for the pressurized o-ring groove side.

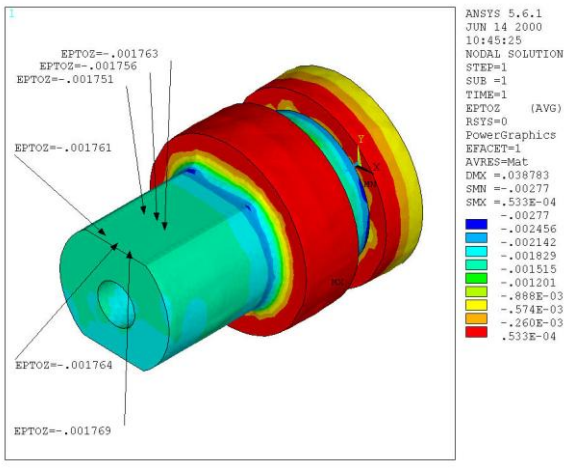

Figure 5. FEM strain results in z-direction at p = 150 MPa for the non-pressurized o-ring groove side.

The results illustrated in figures 4 and 5 shows that the pressure applied on the o-ring groove side until the end of the O-ring groove affected the strain on the strain gauge area by

only a few microstrains. Nonetheless, the stress distribution around the O-ring groove was taken into account during the design of the O-ring groove on the active cylinder. The position of the O-ring on the active cylinder was also analyzed by FEM to understand how it affects the strain and stress distribution on the active element. The 2.6 mm wide O-ring groove was moved ± 2 mm (in z-direction) from its original position (z = 3 mm). At the end of this analysis it has been seen that the strain and stress distribution changed in the area close to the O-ring groove, but it did not really affect the strain in the area where the strain gauges were bonded. The difference in the strain was less than 2 %.

The assumptions listed at the end of the section 1, are generally accepted by those working in the field and it is felt that the error possibly created by the introducing these assumptions should be less than 10 % FS when combined with the discretization error in 3-D FEM.

In section 4, the FEM output results were compared with those derived from the experimental data to see the compatibility.

3. Experimental Measurement

Experimental measurements were performed to validate the FEM output results. Figure 6 shows the setup for the tests and the measurements. Half Wheatstone bridge was used as a measurement circuit. One of the strain gauges located in the axial direction was used with a dummy strain gauge that was bonded on the non-pressurized AISI 4340 steel to measure the axial strain (ε_a). Then, to measure the circumferential strain (ε_c), the other strain gauge located in the radial direction was used with the same dummy gauge.

Figure 6. Photograph of the experimental setup

4. Comparison of the Results and Discussion

The comparison values in table 3 and 4 demonstrate that the numerical and experimental output values are in reasonable agreement (the relative difference is less than 13 % of the full scale) with each other, in view of the mentioned possible sources of error of the numerical and the experimental data. Therefore FEM can be used efficiently for designing purposes.

Table 3. Comparison of the average measured output values with the average of derived FEM strain results for the circumferential strain.

	Measured output ($\mu\varepsilon$)	FEM output ($\mu\varepsilon$)	Rel. difference (% full scale)
p [MPa]	ε_c	ε_c	$\Delta\varepsilon_c$
60	390.9	347.0	4.4
100	664.4	566.0	9.9
150	1006.3	880.0	12.6

The reasons for the difference between the measured and the FEM output strain values can be defined as follows:

- Errors due to the misalignment of the strain gauge during the bonding process and the thickness of the bonding material.
- Errors due to the measuring principle of the strain gauge. The strain in y-direction affects the strain in x-direction and it is not possible to detect the strains both in x and y-direction with the strain gauge at the same time.
- The strain gauges were bonded on a flattened surface. If it were bonded on a cylindrical surface, then the FEM analysis could have been realized in cylindrical coordinate system.

Table 4. Comparison of the average measured output values with the average of derived FEM strain results for the axial strain.

	Measured output ($\mu\varepsilon$)	FEM output ($\mu\varepsilon$)	Rel. difference (% full scale)
p [MPa]	ε_a	ε_a	$\Delta\varepsilon_a$
60	-693.8	-704.0	0.6
100	-1229.9	-1174.0	-3.0
150	-1846.5	-1757.0	-4.9

4. Conclusions

The design, modelling, stress and strain analysis by using the FEM of the manufactured high pressure strain gauge pressure transducer prototypes have been described. The comparison values given in tables 3 and 4 demonstrate that the numerical and experimental output values are in good agreement with each other.

The FEM results illustrated in figures 4 and 5 show that the pressure applied on the O-ring side up to the end of the O-ring groove affected the strain on the area where the strain gages were bonded by only a few microstrains. When we moved the O-ring position 2 mm backwards and forwards from its original position, using the FEM, it was also seen that the stress and strain distribution on the active element in the area closer to O-ring groove changes but it does not significantly affect the strain on the area where the strain gauges were bonded.

Therefore it can be said that the utilization of the FEM can be very supportive for the purposes of designing and optimising the design parameters of such kind of pressure transducers.

The metrological specifications of the constructed pressure transducer prototypes have also been evaluated and reviewed in [5].

Note: The sole purpose of the photograph used in this paper was to identify the measurement setup, it does not represent any form of endorsement of the commercially available equipment.

5.References

[1]. Molinar G., Maghenzani R., and Wisniewski R., 1999. *Free-cylinder strain gauge, pressure transducers up to 2 GPa,*

Physica B Condensed Matter 265, 239-245.

[2]. Molinar G., Bray A., Wisniewski R., Maghenzani R., and Nespoli L., 1998 *Pressure transducer for pressure measurements up to 0.5 GPa*, Measurement 24, 161-172.

[3]. ASM International, 1998. *Heat Treater's Guide*, 2nd Edition, pp. 690-692, USA.

[4]. Micro-Measurements Division, 1992. *Transducer Class®, Strain Gages Bondable Resistors Installation Accessories*, Catalog TC 116-4, Measurements Group, USA

[5]. Orhan M. H., Doğan Ç., Kocabaş H., Tepehan G., *Experimental strain analysis of the high pressure strain gauge pressure transducer and verification by using finite element method*, Measurement Science and Technology, 2001,**12**, 335-344.

[6]. Timoshenko S.P., and Goodier J.N., *Theory of Elasticity*, 3rd edition, 1970. pp. 65-71, Mc Graw-Hill International Editions, Singapore.

[7]. ANSYS Inc., 1998. ANSYS version 5.6 Software Help, Solid 45, USA.

Contact Person for paper:

Haluk Orhan

Address: TUBITAK-Ulusal Metroloji Enstitüsü, P.O.Box:21 41470 Gebze-Kocaeli-TURKEY

Fax:+90 262 646 59 14,

Tel: +90 262 646 63 60